


Cite this: *RSC Adv.*, 2020, 10, 4657

# Comparison of emulsifying capacity of two hemicelluloses from moso bamboo in soy oil-in-water emulsions

Yan-Fei Li,<sup>a</sup> Pan-Pan Yue,<sup>a</sup> Xiang Hao,<sup>ID</sup> \*<sup>a</sup> Jing Bian,<sup>a</sup> Jun-Li Ren,<sup>ID</sup> <sup>b</sup> Feng Peng,<sup>ID</sup> \*<sup>a</sup> and Run-Cang Sun,<sup>ID</sup> <sup>c</sup>

Oil-in-water food emulsions consisting of natural emulsifiers has been an active field of green scientific inquiry. Here, we extract two types of new hemicellulose-based emulsifiers ( $H_H$  and  $H_L$ ) from holocellulose and dewaxed materials of bamboo (*Phyllostachys pubescens*), as well as compare their emulsifying soy oil ability, respectively. The main content of  $H_H$  is arabinoxylan, while the primary composition in  $H_L$  is glucan. The emulsifying capacity of these two types of hemicellulose-based emulsifiers are evaluated by droplet size distribution, surface charge and optical microscopy. Since  $H_L$  possesses higher lignin and protein residual contents, the resultant emulsion exhibits smaller droplets and higher emulsion stability. In comparison,  $H_H$  emulsifier has almost no emulsifying capacity due to the lack of non-polar groups. This study provides insight into the choice of hemicelluloses-based emulsifiers for the formation of stable oil-in-water food emulsions.

Received 22nd October 2019

Accepted 22nd January 2020

DOI: 10.1039/c9ra08636f

rsc.li/rsc-advances

## 1. Introduction

Oil-in-water food emulsions are being developed at a rapid pace because of their many potential applications in food and beverages. In general, they are thermodynamically unstable colloidal systems that need emulsifiers to provide kinetic stability. A large number of emulsifiers have been developed to stabilize food emulsions, including proteins, small colloidal solids, classical monomeric surfactants, and polysaccharides.<sup>1</sup> Given the urgent need for products labelled with clean, demand on the food-grade emulsifier such as polysaccharide grows increasingly. Polysaccharides have properties of thickening and water retention, as well as an emulsification effect on emulsions, due to their hydrophilicity and high molecular weight. The most commonly used polysaccharide emulsifiers in food emulsions are gum arabic, fenugreek, galactomannans, starch, and cellulose derivatives.<sup>2,3</sup> Recent years have witnessed a rapid development on these polysaccharide emulsifiers derived from nature, whereas they are still relatively few compared to synthetic emulsifiers.

In general, there are four factors that affect the emulsifying capacity, including molecular weight, branching degree, the number of lipophilic groups, and protein content. First, the

high molecular weight as well as branching degree of polysaccharides plays the role of emulsifying capacity through steric hindrance and charge repulsion.<sup>4,5</sup> Then, polysaccharides from nature generally have lipophilic groups such as acetyl groups or methoxy groups.<sup>6</sup> These lipophilic groups adsorb to the surface of the oil droplets, thereby achieving the emulsification effect. For example, phenolic residues in spruce galactoglucomannans improve the stability of oil-in-water emulsions.<sup>7</sup> In addition, there are physical and chemical interactions between proteins and polysaccharides, thus proteins cannot be completely removed during the extraction and purification of polysaccharides. The emulsifying and stabilizing ability of the polysaccharides are considered to achieve by introducing an amphiphilic residual protein fraction, increasing the steric repulsion and/or the viscosity of the continuous phase. It should be noted that the stability of emulsifiers is also affected by many factors such as heat variability of free proteins and sensitivity to pH. Consequently, even as emulsifiers derived from polysaccharides, there is a need for more research on extracting, characterizing and clarifying the properties of polysaccharide-based emulsifiers from natural sources in a controlled manner.

Among these polysaccharide emulsifiers, hemicelluloses are heteropolysaccharides that they divided into four types, such as xyloglucans, xylans,  $\beta$ -glucans with mixed linkages, and mannans. Unlike starch and cellulose, hemicelluloses derivatives have lower industrial utilization due to low molecular weight and varying chemical composition.<sup>8</sup> Recently, some researchers have tried to exploit the hemicelluloses-based materials to the food emulsion field. For example, Mikkonen

<sup>a</sup>Beijing Key Laboratory of Lignocellulosic Chemistry, Beijing Forestry University, Beijing 100083, China. E-mail: Xianghao@bjfu.edu.cn; fengpeng@bjfu.edu.cn

<sup>b</sup>State Key Laboratory of Pulp and Paper Engineering, South China University of Technology, Guangzhou 510640, China

<sup>c</sup>Center for Lignocellulose Science and Engineering, Liaoning Key Laboratory Pulp and Paper Engineering, Dalian Polytechnic University, Dalian 116034, China



*et al.*<sup>9</sup> compared the emulsifying and stabilizing capacities of spruce galactoglucomannans (GGM) and its carboxymethyl derivative (CMGGM) with those of known stabilizers, namely, corn fiber gum (CFG) and gum arabic (GA), the latter of which is the gold standard in food emulsions. They demonstrated that GGM and CMGGM were capable of forming emulsions with an average droplet size of approximately 400 nm and stabilizing droplets more effectively than GA. The wood-derived natural emulsifiers GGM and CMGGM exhibited the outstanding emulsification properties, which suggested that hemicelluloses-based material would be potential candidates as emulsifiers for the food industry.

Although some hemicelluloses have been successfully utilized to stabilize oil-in-water food emulsions, most of them are still limited to spruce GGM. Reports on the other types of hemicelluloses to apply in food emulsions are few. In this study, we extract the water-soluble hemicelluloses ( $H_H$  and  $H_L$ ) from holocellulose and dewaxed powder of the bamboo culms, and then examine their emulsifying properties in food emulsions, respectively. The sugar compositions of hemicelluloses are determined by high performance anion exchange chromatography (HPAEC). The lignin and protein residual contents of hemicelluloses are investigated by Klason lignin and the Coomassie brilliant blue G250 (CBBG) methods, respectively. Further, the emulsifying capacity of  $H_H$  and  $H_L$  for the formation of oil-in-water soy oil emulsions are studied by droplet size distribution, zeta-potential, and morphology analysis. Meanwhile, the role of protein and lignin content in hemicelluloses is described. The results obtained may contribute to choosing appropriate hemicelluloses-based emulsifiers for application in the food and beverage industries.

## 2. Material and methods

### 2.1. Materials and chemicals

Moso bamboo (*Phyllostachys pubescens*) was obtained from a local bamboo factory (Sichuan, China). First, it was dried in sunlight and then cut into small pieces (1–3 cm). The chips were dried in sunlight and then grounded to pass a 0.8 mm screen. After being further dried again in a cabinet oven for 16 h at 60 °C. The fats, waxes, and oils of bamboo powder were removed in a Soxhlet apparatus for 6 h with acetone, and the dewaxed bamboo was obtained. All standard chemicals were analytical grade.

### 2.2. Extraction of $H_H$ and $H_L$

The water-soluble hemicelluloses ( $H_L$  and  $H_H$ ) were obtained from the dewaxed bamboo and the delignified bamboo (holocellulose), respectively. The dewaxed bamboo was soaked in distilled water at 80 °C for 8 h with solid-to-liquid ratio of 1 : 20 (g/mL). After filtration, the filtrate was evaporated under reduced pressure and freeze-dried to obtain the water-soluble hemicelluloses, labelled as  $H_L$ . The holocellulose was obtained by delignification of the dewaxed bamboo (40–60 mesh) with 6 wt% sodium chlorite in acidic solution (pH 3.6–3.8, adjusted by 10 wt% acetic acid) at 75 °C for 2 h. The

holocellulose was subsequently extracted with distilled water at 80 °C for 8 h with solid-to-liquid ratio of 1 : 20 (g/mL). After filtration, the filtrate was evaporated under reduced pressure and freeze-dried to obtain water-soluble hemicelluloses, labelled as  $H_H$ .

### 2.3. Chemical characterization

The lignin content of the hemicelluloses was determined by Klason lignin.<sup>10</sup> The protein content of the  $H_L$  and  $H_H$  was determined by the Coomassie brilliant blue G250 (CBBG).<sup>11</sup> The composition of neutral sugars and uronic acids in the hemicelluloses was determined by high performance anion exchange chromatography (HPAEC). The neutral sugars and uronic acids in the  $H_L$  and  $H_H$  were liberated by hydrolysis with 10 wt%  $H_2SO_4$  for 2.5 h at 105 °C. After hydrolysis, the sample was diluted 50 times, filtered, and injected into the HPAEC (Dionex ISC 3000, USA) system with amperometric detector, AS50 autosampler and a Carbowac™ PA1 column (4 mm × 250 mm, Dionex).<sup>10</sup>

### 2.4. Preparation of the emulsions

A series of aqueous emulsifier solutions at different concentrations (0.5 wt%, 1 wt%, 1.5 wt%, 2 wt%, and 2.5 wt%) were prepared by dispersing  $H_H$  and  $H_L$  in 25 mM citrate buffer (pH 4.5) containing 0.05 w/v potassium sorbate as antimicrobial preservative, and stirred overnight at room temperature (RT). Oil-in-water emulsions were prepared by homogenizing 10 wt% oil phase (soy oil) with 90 wt% aqueous phase. A coarse emulsion was prepared by blending oil and aqueous phases together using a high shear mixer (Ouhor Mechanical Equipment Co., Ltd, Homogenizer, Shanghai) for 4 min at ambient temperature. Fine emulsions were formed by a high pressure homogenizer (Microfluidizer LV1, Microfluidics Inc., Newton, MA). The emulsions were stored at RT.

### 2.5. Droplet size

The droplet size distribution of the emulsions was determined with static light scattering, using a Mastersizer Hydro 2000 SM (Malvern Instruments Ltd, Worcestershire, UK). The analysis was repeated five times with fresh emulsions and after 1 h, 1 day, 1 week, 2 weeks, and 1 month storage at RT. Refractive indexes of 1.33 for water and 1.47 for dispersed phase were used. Three measurements on each sample were performed. The emulsions were gently turned upside down 10 times before sampling. Emulsions were diluted with buffer solutions of the appropriate pH before analysis to avoid multiple scattering effects. Dilution was necessary to avoid multiple scattering effects, even though this step might disrupt the emulsion system.<sup>12</sup> The droplet diameter of each sample was represented as the volume-weighted mean diameter ( $D_{4,3}$ ) or surface-weighted mean diameter ( $D_{3,2}$ ), which was calculated from the full droplet size distribution.

### 2.6. Zeta-potential measurement

Zeta-potential was determined using Zetasizer 90 (Malvern Instruments Ltd, USA). All measurements were carried out



according to the method described with slight modifications.<sup>13</sup> For zeta-potential measurement, emulsions were diluted to 0.05 wt% using 25 mM citrate buffer at pH 4.5. Diluted emulsions were injected into a high concentration vial specifically designed for zeta-potential. For measurement of droplet size, the emulsion samples were diluted to approximately 0.005 wt% using 25 mM citrate buffer (pH 4.5). All determinations were conducted in duplicate.

### 2.7. Optical microscopy

The emulsion morphology was characterized using optical microscopy (AxioScope A1, Carl Zeiss Inc., Oberkochen, Germany). Before tested, the emulsion was mixed gently by turning the container upside down ten times.

## 3. Results and discussion

### 3.1. Composition study of $H_L$ and $H_H$

Since the lignin or protein cannot be completely removed during the extraction and purification of polysaccharides, we study the lignin and protein residual content of  $H_H$  and  $H_L$ , as can be seen in Fig. 1a. The lignin content of  $H_L$  and  $H_H$  was determined as 25.50 wt% and 0.67 wt%, respectively. In addition,  $H_L$  possessed much higher protein content with 9.53%, while  $H_H$  only consisted of 0.90 wt% protein. Taken together,  $H_L$  extracted from dewaxed materials of bamboo had much more lignin or protein residual contents.

After confirming the residual contents, we next investigated the sugar composition of these two types of hemicelluloses. As shown in Fig. 1b, the sugar compositions of the  $H_H$  were determined as 75.3 mol% xylose, 15.0 mol% arabinose, 7.0 mol% glucose, and 2.7 mol% galactose, which indicated that the main content of hemicelluloses was arabinoxylan. As for  $H_L$ , the sugar compositions have been measured as 48.5 mol% glucose, 20.4 mol% galactose, 17.9 mol% arabinose, 10.9 mol% xylose, and 2.3 mol% glucuronic acid, suggesting the main content of glucan. Since the glucan was the main component of  $H_L$ , we reasoned that the  $H_L$  obtained from dewaxed materials of bamboo contained starch.<sup>14</sup>

FT-IR study was further conducted to confirm the composition of  $H_H$  and  $H_L$  (Fig. 2). Both of  $H_H$  and  $H_L$  showed obvious absorption at  $3408\text{ cm}^{-1}$  and  $2939\text{ cm}^{-1}$ , which were attributed to the O–H stretching vibration of the hydroxyl groups and C–H ( $\text{CH}_2$  and  $\text{CH}_3$ ) stretching vibrations in hemicelluloses,<sup>15</sup> respectively. The FT-IR spectra also demonstrated that the hemicelluloses can be obtained from holocellulose without cleaving the acetyl ester groups by the treatment with water, in which the absorption around  $1736\text{ cm}^{-1}$  represented the C=O stretching of acetyl groups in the region of the carbonyl stretching vibration. In terms of  $H_H$ , the band at  $1736\text{ cm}^{-1}$  was ascribed to xylan, whereas it cannot be found in the spectrum of  $H_L$ . In addition, the stretching modes around  $1240\text{ cm}^{-1}$  and  $1249\text{ cm}^{-1}$  were assigned to the C–O linkage in xylan.<sup>16</sup> Evidently, these bands in the spectrum of  $H_H$  were much stronger than those of  $H_L$ . As for  $H_L$ , the characteristic bands at  $1598\text{ cm}^{-1}$ ,  $1509\text{ cm}^{-1}$ , and  $1412\text{ cm}^{-1}$  were exploited to

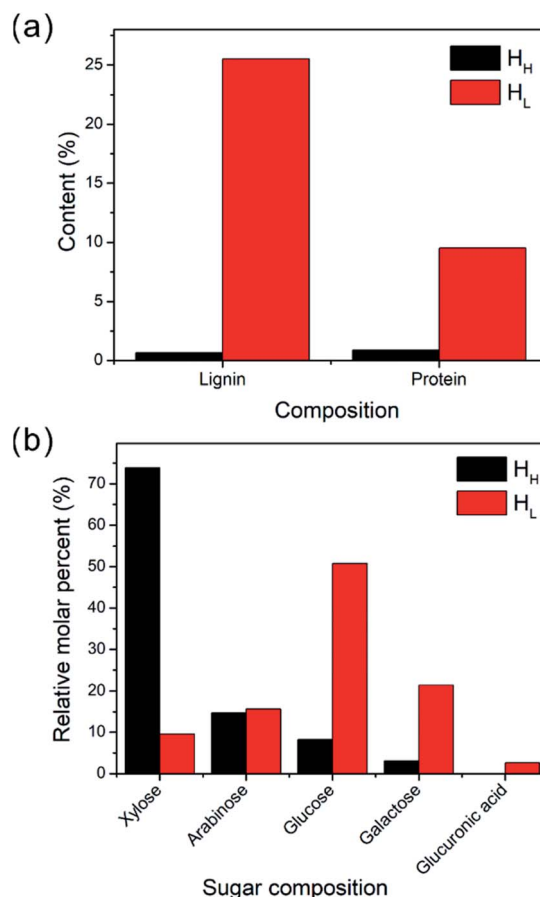


Fig. 1 (a) The lignin and protein composition of  $H_H$  and  $H_L$ . (b) Sugar composition analysis of  $H_H$  and  $H_L$ .

confirm the presence of lignin, since they were not overlapped with bands from carbohydrates.<sup>17</sup> In comparison, the absence of band at  $1509\text{ cm}^{-1}$  in the  $H_H$  spectrum implied that few lignin existed in  $H_H$ , which was in accordance with the result of the

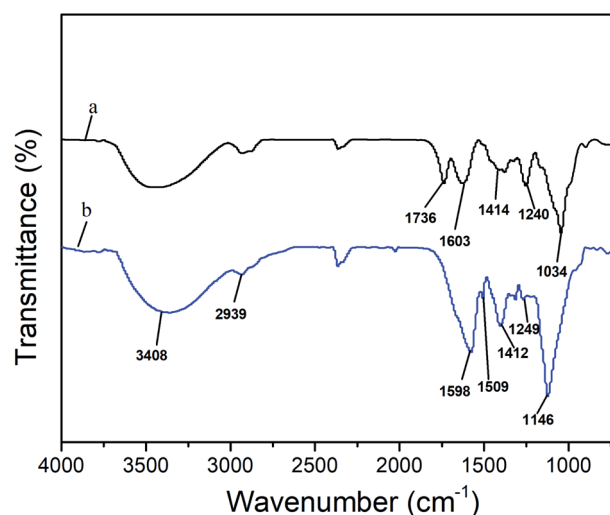


Fig. 2 FT-IR spectra of (a)  $H_H$  and (b)  $H_L$ , respectively.

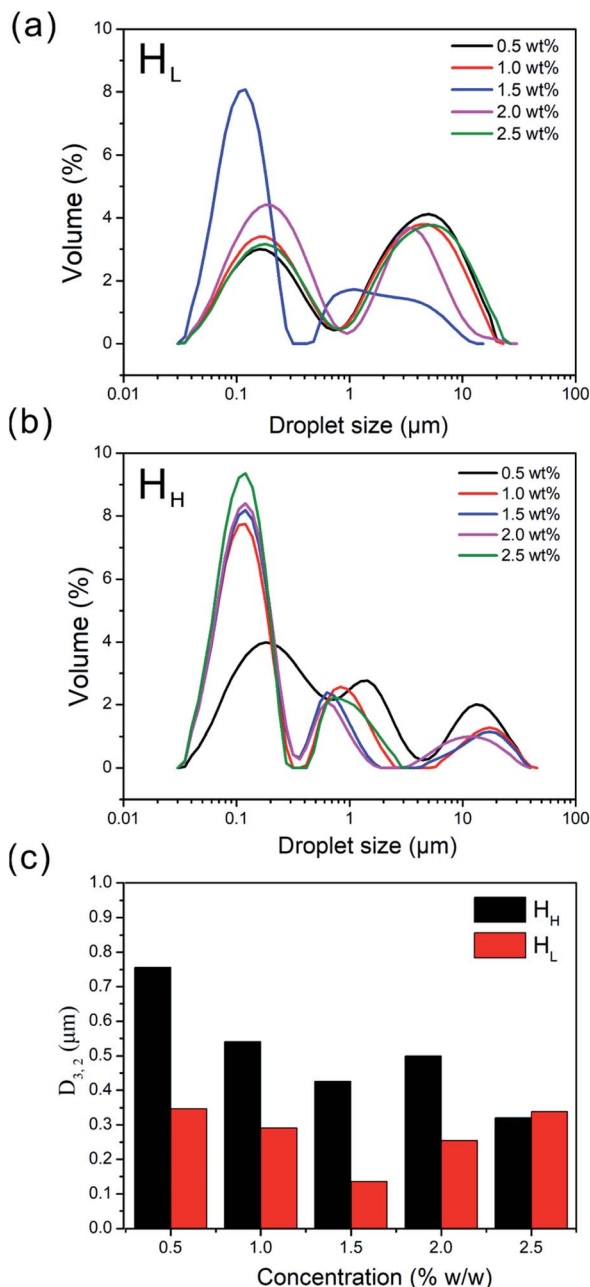


Fig. 3 Droplet size distribution as a function of concentration of (a)  $H_L$  and (b)  $H_H$  for oil-in-water emulsions. (c) Comparison of the droplet size  $D_{3,2}$  for emulsions containing different concentration of  $H_H$  and  $H_L$ .

composition of  $H_H$ . Evidently, this peak in the spectrum of  $H_H$  was stronger than that of  $H_L$ . The peaks at  $1034\text{ cm}^{-1}$  and  $1146\text{ cm}^{-1}$  seem to be due to the C-OH bending mode and C-O stretching in C-O-C glycosidic linkages, respectively.<sup>10</sup>

### 3.2. Emulsifying capacity evaluation

**3.2.1. Influence of hemicelluloses type and concentration on the droplet size distribution.** The droplet size distributions of the emulsions formed by  $H_L$  and  $H_H$  were determined to gain insight into emulsifying capacity. The influences of emulsifier

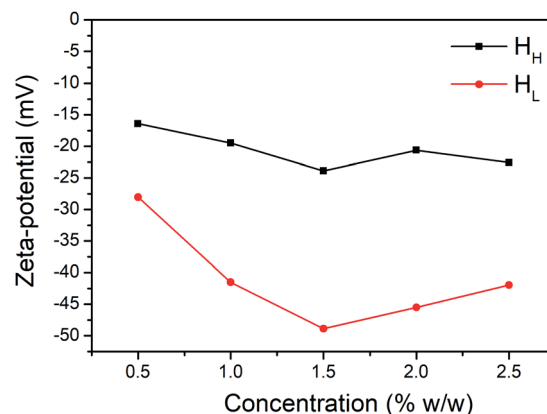


Fig. 4  $\zeta$  of  $H_H$ -stabilized and  $H_L$ -stabilized emulsions as a function of emulsifier concentration.

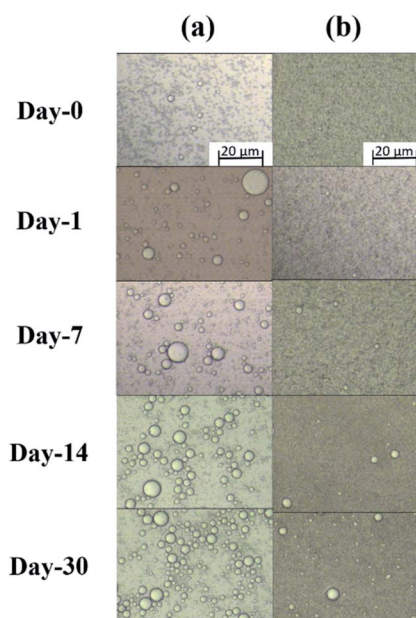


Fig. 5 Optical micrographs of emulsions with 10 wt% soy oil stabilized with 1.5 wt% (a)  $H_H$  and (b)  $H_L$  at different storage times, respectively. The scale bar is 20  $\mu\text{m}$ , and all images were at the same magnification.

concentration on droplet size distribution for the formation of oil-in-water emulsions were depicted in Fig. 3a–c. All of these emulsions displayed multimodal droplets size distributions. The droplet size distribution of  $H_L$ -stabilized emulsions displayed double peak and  $H_H$ -stabilized emulsions displayed triple peak in Fig. 3a and b. In terms of  $H_L$ -stabilized emulsion, the size distribution was prone to displaying monomodal as the concentration of  $H_L$  increased from 0.5 wt% to 1.5 wt%. If the concentration was further increased to 2.5 wt%, the heterogeneity appeared again with the increasing of larger droplets size. A proportion of  $H_L$  were not adsorbed on the surface of the oil droplets with the high concentration emulsion system. The increased viscosity produced depletion interaction in the emulsions to bring about the migration of oil droplets through





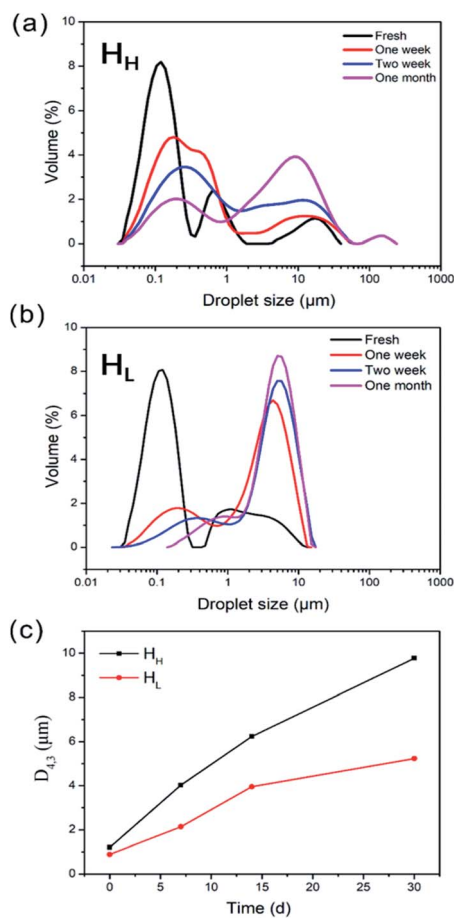


Fig. 6 Effect of time on the droplet size distributions with 10 wt% soy oil stabilized with 1.5 wt% (a)  $H_H$  and (b)  $H_L$ . (c) Partial size  $D_{3,2}$  of emulsions with 10 wt% soy oil stabilized with 1.5 wt%  $H_H$  and  $H_L$  emulsifiers.

the continuous phase. The droplets approached further to form larger droplets. It was found that 1.5 wt% emulsions can form smaller droplets compared to other concentration. Similar trend were observed by Long *et al.*,<sup>18</sup> in which emulsifier concentration has a great effect on the stability of the emulsions. The droplet surfaces were not effectively covered by emulsifiers, when the emulsifier concentration reached a certain level. In comparison, the  $H_H$ -stabilized emulsions exhibited rather inhomogeneity with multimodal droplet size distributions (Fig. 3b). Besides, the diameter distribution of oil droplets can be improved with the increase of the  $H_H$  concentration, while the effect of  $H_H$  was not comparable to that of  $H_L$ .

Emulsions were prepared by mixing soy oil and emulsifiers solutions with different emulsifier concentration at room temperature, and then the surface-weighted mean diameter ( $D_{3,2}$ ) was measured after 1 h (Fig. 3c). As shown in Fig. 3c, the  $D_{3,2}$  of  $H_H$ -stabilized emulsions was always larger than those of  $H_L$ -stabilized emulsions in the concentration ranging from 0.5 wt% to 2.0 wt%. Specifically, the  $D_{3,2}$  of the  $H_L$ -stabilized emulsions dropped at first and then rose with increasing emulsifier concentration, which suggested that the smallest surface-weighted mean diameter is existed at 1.5 wt%

concentration. More emulsifier molecules were adsorbed at the oil-water interface with the increasing of emulsifier concentration, which reduced interfacial free energy in the dispersion system, thereby oil droplets were more difficult to coalesce. However, the increased viscosity caused depletion interaction in a high concentration system and the excess emulsifier in the continuous phase increased the attractive force between the droplets by osmotic effect, whereby the chains of polysaccharides were excluded from the narrow region surrounding the two droplets,<sup>19</sup> so that the droplets size increased. In comparison, the  $D_{3,2}$  of the  $H_H$ -stabilized emulsions displayed a bigger value than that of  $H_L$ . It indicated that the  $H_H$ -stabilized emulsions contained much larger droplets than  $H_L$ -stabilized emulsions.

**3.2.2.  $\zeta$ -potential study.** Zeta-potential ( $\zeta$ ) is an important indicator to characterize the stability of the dispersion system. In general, the greater value of the absolute  $\zeta$  value, the greater repulsive force between the droplets, resulting in the enhancement the stability of emulsion. The surface potential results showed that  $\zeta$  of all the emulsions had negative values, wherein the absolute  $\zeta$  value of the  $H_L$ -stabilized emulsion was larger than that of the  $H_H$ -stabilized emulsion (Fig. 4). As for  $H_L$ -stabilized emulsion, the zeta-potential decreased from  $-28.06$  mV to  $-48.84$  mV with concentration increasing from 0.5 wt% to 1.5 wt%, followed by an increase from  $-48.84$  mV to  $-41.94$  mV with the  $H_L$  concentration increasing to 2.5 wt%. Besides, the absolute  $\zeta$  value of the  $H_L$ -stabilized emulsion was larger than that of the  $H_H$ -stabilized emulsion, confirming the stability of the  $H_L$ -stabilized emulsion. The discrepancy on emulsifying capacity could be attributed to the specific composition of  $H_L$ . Before the concentrations of  $H_L$  reaching optimum, more lipophilic group of  $H_L$  emulsifier would absorb on the droplet interface. Non-absorbed polysaccharides are most likely responsible for promoting droplet flocculation through a depletion mechanism, reducing the chance of mutual coalescence between the oil droplets when the emulsifier was quickly absorbed onto the new oil-water interfaces, thereby making  $H_L$  become an effective emulsifier.<sup>20</sup>

### 3.3. Long-term stability study

**3.3.1. Influence of time on morphology.** Physical stability of emulsions composed of  $H_H$  and  $H_L$  was evaluated by optical microscopy. After emulsifying, small micro-size droplets were observed in both of the two fresh emulsions (Fig. 5), wherein the droplets size of  $H_H$ -stabilized emulsion was larger than that of  $H_L$ -stabilized emulsion. The droplet size became larger with increasing of storage time. After a day, the emulsions were prepared to visualize the existence of droplets smaller than 1 mm that were abundant in the  $H_L$  (Fig. 5b) and  $H_H$  (Fig. 5a) emulsions. There were a number of larger oil droplets in the  $H_H$ -stabilized emulsion, while the larger oil droplets of  $H_L$  stabilized emulsion only slightly increased. With the increased storage time, heterogeneous droplets were observed in  $H_H$ -stabilized emulsion that oil droplet size differences. The  $H_L$ -emulsions also contained some droplets several micrometres in diameter, and the oil phase of the  $H_H$ -emulsions was mainly



composed of such large droplets (Fig. 5a). The visual observation and the microscopy of the emulsions indicated that  $H_L$  enabled the formation of small oil droplets that made the emulsions more stable against creaming than those containing  $H_H$  (Fig. 5).

### 3.3.2. Influence of time on the droplet size distribution.

The droplet size distribution as a function of time for  $H_L$ - and  $H_H$ -stabilized emulsions were evaluated, as shown in Fig. 6a–c. The  $H_L$ -stabilized emulsions showed bimodal droplet size distribution with an increase percentage of large droplet (Fig. 6b). The size distribution of the  $H_H$ -emulsions displayed three peaks after one month (Fig. 6a). In addition, nano-size droplets were dominant in the fresh  $H_L$  and  $H_H$  emulsions, whereas the large micro-droplets became the major part after long time storage. The large droplets developed could also be ascribed to the clusters of droplets, indicating the appearance of flocculates. Despite both emulsions displayed long-term instability, the  $H_L$ -stabilized emulsions was relatively stable than  $H_H$ -stabilized emulsions.

We then investigated the influence of time on the  $D_{4,3}$  of various emulsions, as can be shown in Fig. 6c. After preparation, the  $D_{4,3}$  of  $H_H$ -stabilized emulsion were approach to  $H_L$ -stabilized emulsion with 1.2  $\mu\text{m}$  and 0.9  $\mu\text{m}$ , respectively. However, the  $D_{4,3}$  of  $H_H$ -stabilized emulsions increased faster than that of  $H_L$  with increasing storage time. After one month, the  $D_{4,3}$  of  $H_H$ -stabilized emulsion was increased to  $\sim 10 \mu\text{m}$ , which was larger than that of  $H_L$ -stabilized emulsion with about  $\sim 5 \mu\text{m}$ , confirming the better emulsifying performance of  $H_L$ .

## 4. Conclusions

In summary, we successfully obtain the water-soluble hemicelluloses ( $H_H$  and  $H_L$ ) from holocellulose and dewaxed powder of the bamboo culms, and then compare their emulsifying capacity for oil-in-water food emulsion, respectively. The main content of  $H_H$  is arabinoxylan, while the primary composition in  $H_L$  is glucan. The  $H_L$  type hemicelluloses possess much higher lignin and protein residual content with 25.5 wt% and 9.3 wt%, respectively. In contrast,  $H_H$  only consists of 0.67 wt% protein and 0.9 wt% lignin, respectively. The discrepancy of residual content makes these two type hemicelluloses with different emulsifying property. For soy oil-in-water emulsion, the  $H_L$  type emulsifier displays much better emulsifying performance than  $H_H$ , with relatively uniform size distribution, large  $\zeta$  absolute value and smaller droplet size. In addition, the  $H_L$ -stabilized emulsion shows much long-term stability than  $H_H$ -stabilized emulsion, wherein the  $H_H$ -stabilized emulsion displays seriously flocculation with the lapse of time. Considering the similar non surface-active inherence of glycosyl units, the emulsifying capacity of  $H_L$  is mainly attributed to the non-polar and charge groups brought by the residual content. The findings in this study may provide beneficial information to guide the formation of hemicelluloses-based food emulsion.

## Conflicts of interest

There are no conflicts to declare.

## Acknowledgements

This research was funded by the Fundamental Research Funds for Central Universities (2019ZY05), Beijing Forestry University Outstanding Young Talent Cultivation Project (2019JQ03017), National Natural Science Foundation of China (31971611).

## References

- 1 Z. A. Zell, A. Nowbahar, V. Mansard, L. G. Leal, S. S. Deshmukh, J. M. Mecca, C. J. Tucker and T. M. Squires, Surface shear inviscidity of soluble surfactants, *Proc. Natl. Acad. Sci. U. S. A.*, 2014, **111**, 3677–3682.
- 2 A. C. Karaca, N. H. Low and M. T. Nickerson, Potential use of plant proteins in the microencapsulation of lipophilic materials in foods, *Trends Food Sci. Technol.*, 2015, **42**, 5–12.
- 3 R. S. H. Lam and M. T. Nickerson, Food proteins: a review on their emulsifying properties using a structure-function approach, *Food Chem.*, 2013, **141**, 975–984.
- 4 S. P. Nie, C. Wang, S. W. Cui, Q. Wang, M. Y. Xie and G. O. Phillips, A further amendment to the classical core structure of gum arabic (*Acacia senegal*), *Food Hydrocolloids*, 2013, **31**, 42–48.
- 5 S. P. Nie, C. Wang, S. W. Cui, Q. Wang, M. Y. Xie and G. O. Phillips, The core carbohydrate structure of *Acacia seyal* var. *seyal* (Gum arabic), *Food Hydrocolloids*, 2013, **32**, 221–227.
- 6 E. Dickinson, Hydrocolloids at interfaces and the influence on the properties of dispersed systems, *Food Hydrocolloids*, 2013, **17**, 25–39.
- 7 M. Lehtonen, S. Teräslahti, C. Xu, M. P. Yadav, A. Lampi and K. S. Mikkonen, Spruce galactoglucomannans inhibit lipid oxidation in rapeseed oil-in-water emulsions, *Food Hydrocolloids*, 2016, **58**, 255–266.
- 8 K. S. Mikkonen and M. Tenkanen, Sustainable food-packaging materials based on future biorefinery products: xylans and mannans, *Trends Food Sci. Technol.*, 2012, **28**, 90–102.
- 9 K. S. Mikkonen, C. Xu, C. Berton-Carabin and K. Schroën, Spruce galactoglucomannans in rapeseed oil-in-water emulsions: efficient stabilization performance and structural partitioning, *Food Hydrocolloids*, 2016, **52**, 615–624.
- 10 F. Peng, J. L. Ren, F. Xu, J. Bian, P. Peng and R. C. Sun, Fractionation of Alkali-Solubilized Hemicelluloses from Delignified *Populus gansuensis*: Structure and Properties, *J. Agric. Food Chem.*, 2010, **58**, 5743–5750.
- 11 Q. Q. Liang and Y. S. Li, A rapid and accurate method for determining protein content in dairy products based on asynchronous-injection alternating merging zone flow-injection spectrophotometry, *Food Chem.*, 2013, **141**, 2479–2485.
- 12 L. Q. Zou, B. J. Zheng, W. Liu, C. M. Liu, H. Xiao and D. J. McClements, Enhancing nutraceutical bioavailability using excipient emulsions: influence of lipid droplet size



- on solubility and bioaccessibility of powdered curcumin, *J. Funct. Foods*, 2015, **15**, 72–83.
- 13 Y. S. Gu, E. A. Decker and D. J. McClements, Formation of colloidosomes by adsorption of small charged oil droplets onto the surface of large oppositely charged oil droplets, *Food Hydrocolloids*, 2007, **21**, 516–526.
  - 14 B. Zhang, Y. Guan, J. Bian, F. Peng, J. L. Ren, C. L. Yao and R. C. Sun, Structure of hemicelluloses upon maturation of bamboo (*Neosinocalamus affinis*) culms, *Cellul. Chem. Technol.*, 2016, **50**, 189–198.
  - 15 B. Zhang, G. Q. Fu, Y. S. Niu, F. Peng, C. L. Yao and R. C. Sun, Variations of lignin-lignin and lignin-carbohydrate linkages from young *Neosinocalamus affinis* bamboo culms, *RSC Adv.*, 2016, **6**, 15478–15484.
  - 16 P. P. Yue, Y. J. Hu, G. Q. Fu, C. Sun, M. Li, F. Peng and R. C. Sun, Structural Differences between the Lignin-Carbohydrate Complexes (LCCs) from 2- and 24-Month-Old Bamboo (*Neosinocalamus affinis*), *Int. J. Mol. Sci.*, 2018, **19**, 1.
  - 17 P. P. Yue, G. Fu, Y. Hu, J. Bian, M. Li, Z. Shi and F. Peng, Changes of Chemical Composition and Hemicelluloses Structure in Differently Aged Bamboo (*Neosinocalamus affinis*) Culms, *J. Agric. Food Chem.*, 2018, **66**, 9199–9208.
  - 18 L. Bai, S. Q. Huan, Z. G. Li and D. J. McClements, Comparison of emulsifying properties of food-grade polysaccharides in oil-in-water emulsions: gum arabic, beet pectin, and corn fiber gum, *Food Hydrocolloids*, 2017, **66**, 144–153.
  - 19 D. J. McClements, Comments on viscosity enhancement and depletion flocculation by polysaccharides, *Food Hydrocolloids*, 2000, **14**, 173–177.
  - 20 F. Donsì, M. Sessa and G. Ferrari, Effect of Emulsifier Type and Disruption Chamber Geometry on the Fabrication of Food Nanoemulsions by High Pressure Homogenization, *Ind. Eng. Chem. Res.*, 2011, **51**, 7606–7618.

